Synthesis and Characterization of CaTiO3-LnAlO3(Ln=La, Nd) Ceramics Manufactured by Reaction Sintering Method

Shicheng Zhou
Guilin University of Technology
Qiang Wu
Guilin University of Technology
Hanrui Xu
Guilin University of Technology
Xiaowen Luan
Guilin University of Technology
Sang Hu
Guilin University of Technology
Xianjie Zhou
Guilin University of Technology
Sen He
Guilin University of Technology
Xi Wang
Guilin University of Technology
Hailin Zhang
Guilin University of Technology
Xiuli Chen
Guilin University of Technology
Huanfu Zhou (zhouhuanfu@163.com)
Guilin University of Technology

Research Article

Keywords: CaTiO3-LnAlO3(Ln=La, Nd) ceramics, Reaction sintering method, Microwave dielectric properties

Posted Date: April 7th, 2021

DOI: https://doi.org/10.21203/rs.3.rs-395144/v1

Synthesis and characterization of $CaTiO_3$-$LnAlO_3$(Ln=La, Nd) ceramics manufactured by reaction sintering method

Shicheng Zhou[†], Qiang Wu[†], Hanrui Xu, Xiaowen Luan, Sang Hu, Xianjie Zhou, Sen He, Xi Wang, Hailin Zhang, Xiuli Chen, Huanfu Zhou[*].

Collaborative Innovation Centre for Exploration of Hidden Nonferrous Metal Deposits and Development of New Materials in Guangxi, Key Laboratory of Nonferrous Materials and New Processing Technology, Ministry of Education, School of Materials Science and Engineering, Guilin University of Technology, Guilin 541004, China.

Abstract

$CaTiO_3$-$LnAlO_3$(Ln=La, Nd) ceramics were manufactured by reaction-sintering for produce low cost and high efficiency materials. Using reaction-sintering method to manufacture these ceramics, which have excellent comprehensive properties. The subtle variations on densification behavior, phase transformation, phase composition, microstructure evolution and performances of $CaTiO_3$-$LnAlO_3$(Ln=La, Nd) ceramics were studied systematically. The XRD pattern indicates that the $Ca_{0.61}La_{0.39}Al_{0.39}Ti_{0.61}O_3$ phase and $Ca_{0.7}Nd_{0.3}Ti_{0.7}Al_{0.3}O_3$ phase were generated under certain environmental conditions respectively. The ceramics exhibited excellent performance parameters: when ε_r is 42.03(45 635), the quality factor is 45500GHz (45 635) In addition, even in the environment of large temperature changes the ceramics can still maintain good performance. In conclusion, the reaction sintering method is an economic, convenient, available preparation means of making the $CaTiO_3$-

[†] These authors have equal contribution to this work
[*] Corresponding author, E-mail: zhouhuanfu@163.com

$LnAlO_3$(Ln=La, Nd) ceramics and has broad prospects of application and development.

Keywords: $CaTiO_3$-$LnAlO_3$(Ln=La, Nd) ceramics; Reaction sintering method; Microwave dielectric properties

1. Introduction

The wireless communication industries led by microwave communication technology are developing at a rapid pace. A better and serious request about the performance of the functional ceramics was also put forward by this prospect.[1-3]. Because of smallness, lightness, and cheapness microwave dielectric ceramics are excellent candidate materials for communication technologies [4-6].

In actual application, process flow and production cost are factors that must be considered. High production expenses will limit the prospect of numerous microwave ceramics, as $(1-x)ZnNb_2O_6$-xBa$(Zn_{1/3}Nb_{2/3})O_3$[7]. For the sake of practical application, appropriate raw materials and efficient processes are necessary. Suvorov *et al.* reported that although the $CaTiO_3$ ceramics demonstrate favorable microwave dielectric properties (ε_r = 170), its practical application is hindered by quality factor ($Q\times f$ = 3500 GHz) and temperature coefficient (τ_f = +800 ppm/°C). It is easy to acquire useful microwave dielectric ceramics via synthesizing two perovskite structure compounds together[8]. $CaTiO_3$-$LnAlO_3$(Ln=La, Nd) solid solution ceramics exhibited good performances, which preserves excellent comprehensive properties: ε_r 37~44, $Q\times f$ 41 000~47 000GHZ, τ_f -1.5~6ppm/°C. Ravi *et al.* reported that 0.7$CaTiO_3$-0.3$LaAlO_3$ ceramics doped with 0.25wt% Al_2O_3 sintered at 1500°C, and the ceramic showed great performance parameters: ε_r = 46, $Q\times f$ = 38 289 GHz, and τ_f = +12 ppm/°C[9].

In this work, using reaction sintering method to manufacture $CaTiO_3$-$LnAlO_3$(Ln=La, Nd) ceramics to simplify experimental procedures and optimize the dielectric properties. Also, the solid-state reaction mechanism of the $CaTiO_3$-$LnAlO_3$(Ln=La, Nd) solid solution was also investigated, which determine the origin

of the intermediate phase.

2. Materials and methods

$CaTiO_3$-$LnAlO_3$(Ln=La, Nd) ceramic samples were made from high purity materials(≥99%) including $CaCO_3$, TiO_2, Al_2O_3, La_2O_3, and Nd_2O_3, therefore pre-processing of high purity raw materials is the foremost section in fabrication of high quality dielectric ceramics, especially La_2O_3, and Nd_2O_3. Put La_2O_3, and Nd_2O_3 into muffle furnace at 900℃ for two hours respectively, and the mole ratios of $CaTiO_3$-$LaAlO_3$ and $CaTiO_3$-$NdAlO_3$ were determined to be 0.675:0.325 and 0.695:0.305, respectively. The powder was blended with zirconia pellets in alcoholic medium for 4 h. After drying in an oven, samples in cylindrical molds with a diameter of 10mm and a height of 5mm were fabricated at 20 MPa. Finally, they have been sintered from 1475℃ to 1575℃ with a gradient of 25℃ for 6 h respectively.

Using the X-ray diffraction (Model X'Pert PRO, PANalytical, Almelo, Holland) with Cu K_α radiation at 40 kV and 40 mA ($5° \leq 2\theta \leq 80°$) to analyze the microstructure and crystalline of the ceramics. The surface topography and crystal size were observed with SEM (Model JSM6380-LV SEM, JEOL, Tokyo, Japan). Performance parameters of specimens were acquired by using the network analyzer (Model E5071 CENA, Agilent Co, California, USA, 300KHz-20GHz). The τ_f values of the samples were measured from the resonant frequencies at 25 °C to 85 °C and was defined as:

$$t_f = (f_2 - f_1)/f_1(T - T_0) \quad (1),$$

where f_2 and f_1 are the resonance frequencies at 85 °C and 25 °C, respectively.

3. Results and discussion

Figure 1 presents the XRD spectrum of CTLA and CTNA samples sintered from 1100 to 1575°C for 6h, respectively. As shown in Fig1(a), the XRD spectrum of the CTLA samples revealed that there are two types of phase $CaTiO_3$(PDF #96-900-2802) and $LaAlO_3$(PDF #01-082-0478) at 1100°C. As the temperature is 1475°C, two phases are completely form a solid solution. All diffraction peaks are homogeneous $Ca_{0.61}La_{0.39}Al_{0.39}Ti_{0.61}O_3$ main phase, corresponding to the tetragonal perovskite structure (PDF: 00-052-1773), belonging to the $P4_22_12$ space group[10]. The tendency of Fig1(b) is similar as Fig1(a). The ceramic specimen was composed of both $CaTiO_3$ and $NdAlO_3$ phases, and the secondary phase gradually disappeared at 1200°C[11]. Upon further increase of the temperature to 1450 °C, the main peak of the CTNA ceramics appeared at 2θ = 33.2°, which matches well with the 2θ value of the $Ca_{0.7}Nd_{0.3}Ti_{0.7}Al_{0.3}O_3$ phase (PDF: 96-153-3888), belonging to the Pnma space group[12-14]. Using the GASA software could further enhance the fitting accuracy and ascertain the cation position of the samples accurately, the refinement results are shown in Fig. 2. Both samples exhibited a single $CaTiO_3$ phase with a orthorhombic structure in the Pbmn model, and the lattice parameters of this ceramic are as follows: a = 5.358(6)Å, b = 7.593(10) Å, c = 5.394(5) Å, and $\alpha = \beta = \gamma = 90°$. The small R-values (CTLA: Rp = 4.09%, Rwp = 7.43%; CTNA: Rp = 4.17%, Rwp = 7.57%) manifest that the XRD result matched faultlessly consistent with $CaTiO_3$ (PDF: 75-0437) with orthorhombic structure, which indicates that CTLA and CTNA ceramics are fused to form a complete solid solution. Ca^{2+}, La^{3+}, Nd^{3+} take up the A-site of the oxygen octahedron, and Ti^{4+}, Al^{3+} take up the B-site of the oxygen octahedron[15, 16].

Figure 3 shows the SEM micrographs of $CaTiO_3$-$LnAlO_3$(Ln=La, Nd) samples sintered at various temperatures. The micromorphology is variable with the changing of temperature. When the sintering temperatures were less than 1450°C, the particles are composed of small crystal and the structure is not dense enough, which manifest that low temperature cannot provide enough energy for grain growth[17-19]. Raising the temperature again the samples surface becomes more compact and homogeneous and few grain boundaries appears. When the sintering temperature exceeds 1525°C, there were only a few pores in the sample[20, 21]. The above results shown that $CaTiO_3$-$LnAlO_3$(Ln=La, Nd) ceramics could keep excellent performance in a wide temperature range. Using EDS to verify the molar ratios of elements in $CaTiO_3$-$LnAlO_3$(Ln=La, Nd) ceramics, which verifies the analysis and conclusion of XDR. Table 1includes the results of EDS in detail. All samples contain only Ca, Ti, Al, La/Nd and O elements. The calculated result of Ca/Al atomic number ratio is same with the main crystal phase. For example, the atomic number ratio of Ca/Ti to Nd/Al is close to 7:3 in CTNA ceramics, which is very consistent with the stoichiometric ratio of $Ca_{0.7}Nd_{0.3}Ti_{0.7}Al_{0.3}O_3$ phase.

Fig.4 including the curves of ρ, ε_r, $Q\times f$ and τ_f of $CaTiO_3$-$LnAlO_3$(Ln=La, Nd) ceramics with the changing of the sintering temperature. The bulk densities of CTLA and CTNA ceramics were 4.47–4.68 g/cm^3 and 4.48–4.80 g/cm^3. With the rise of temperature ,the bulk densities ρ of CTNA ceramics and CTLA ceramics firstly rose due to the growth of grains, reaching the maximum values at a selected temperature, and then its density declines gradually due to the inner defects caused by extra-high

temperature. When the temperature gradually increases to the ideal temperature, the ceramic grains grow and discharge the pores inside the ceramic, making microstructure of the ceramic more compact. and reaching the maximum. When the temperature exceeds the optimal temperature, the phenomenon of overburning occurs. The grain growth rate is too fast to discharge the pores inside the ceramic in time, contributing to the decline in the density[22-24].

As the sintering temperature increases, the dielectric constant of $CaTiO_3$-$LnAlO_3$(Ln=La, Nd) ceramics reaches a maximum value at the optimum temperature and then decreases. The trend is similar to the relative density. The high density of ceramics is accompanied by high polarizability and thus to an increase in polarization intensity[2, 25]. The relationship between the dielectric constant and the dielectric polarizability and molar volume fraction of the materials can be explained clearly by the Clausius-Mossotti formula used in the literature as follows:

$$\varepsilon th = \frac{3Vm+8\pi\alpha D}{3Vm-4\pi\alpha D} \quad (2),$$

where *Vm* is the cell volume of the $Ca_{0.61}La_{0.39}Al_{0.39}Ti_{0.61}O_3$ and $Ca_{0.7}Nd_{0.3}Ti_{0.7}Al_{0.3}O_3$ molecule, and α is their polarization rates. The total ion polarization rate of $Ca_{0.61}La_{0.39}Al_{0.39}Ti_{0.61}O_3$ and $Ca_{0.7}Nd_{0.3}Ti_{0.7}Al_{0.3}O_3$ can be calculated as follows:

$$\alpha(Ca_{0.61}La_{0.39}Al_{0.39}Ti_{0.61}O_3)=0.61\alpha(Ca^{2+}) +0.61\alpha(Ti^{4+}) +0.39\alpha(La^{3+}) +0.39\alpha(Al^{3+}) +3\alpha(O^{2-}) \quad 12.4203(3)$$

$$\alpha(Ca_{0.7}Nd_{0.3}Ti_{0.7}Al_{0.3}O_3)=0.7\alpha(Ca^{2+}) +0.7\alpha(Ti^{4+}) +0.3\alpha(Nd^{3+}) +0.3\alpha(Al^{3+}) +3\alpha(O^{2-}) \quad 12.033(4)$$

Where $\alpha(Ca^{2+})=3.16Å^3$,$\alpha(Ti^{4+})=2.93Å^3$,$\alpha(La^{3+})=6.07Å^3$,$\alpha(Nd^{3+})=5.01Å^3$,$\alpha(Al^{3+})=0.79Å^3$ and $\alpha(O^{2-})=2.01Å^3$. The theoretical permittivity of CTLA and CTNA were

40.86 and 31.9, respectively. Due to the high dielectric constant of calcium titanate and the grain priority growth, there is a large difference between the measured and calculated values of ε[26].

There are two types of materials losses at microwave frequency: on the one hand the intrinsic loss mainly determined by the lattice vibration mode could influence the properties of materials, on the other hand the external loss determined by the second phase, oxygen vacancies, grain size and densities could also affect the properties of materials[27, 28]. In the same system, the excellent performance of materials depends on the grain size and the number of pores. Therefore, with increasing temperature, the variation of $Q\times f$ value is close to the dielectric constant, which the maximum $Q\times f$ values of $CaTiO_3$-$LnAlO_3$(Ln=La, Nd) ceramics are 46,269 GHz and 45,635 GHz, respectively. According to the Fig 4, the quality factor of $CaTiO_3$-$LnAlO_3$(Ln=La, Nd) ceramics is greater than 41,000under different ranges of temperature. The τ_f values of $CaTiO_3$-$LnAlO_3$(Ln=La, Nd) ceramics remain stable at -1.5 to 6 ppm/°C no matter how the temperature changes. The fluctuations in their τ_f values are mainly caused by grain size, porosity, oxygen vacancies, etc[29, 30]. These indicate that the $CaTiO_3$-$LnAlO_3$(Ln=La, Nd) ceramics has achieved excellent performance in a wide temperature range.

4. Conclusion

The densification behavior, phase transformation, phase composition, microstructure evolution and performances of $CaTiO_3$-$LnAlO_3$(Ln=La, Nd) have been reported by the reaction-sintering method. Solid-solutions with tetragonal and

orthorhombic perovskite structures were formed. The $CaTiO_3$-$LnAlO_3$(Ln=La, Nd) ceramics exhibited the excellent performances as the temperature is between 1475 and 1575°C. The ceramics sintered at 1500 and 1525°C indicated that it has considerable performance parameters CTNA: $Q\times f$ = 45 635 GHz, ε_r = 39.1, and τ_f = -1.48 ppm/°C; CTLA: $Q\times f$ = 46 269 GHz, ε_r = 44.03, and τ_f = 2.63 ppm/°C). The preparation of $CaTiO_3$-$LnAlO_3$(Ln=La, Nd) ceramics by reaction-sintering method has the advantages of simple preparation process, low preparation cost, and wide sintering temperature range, which showing good prospects for industrial applications.

Acknowledgment

This work was supported by the Natural Science Foundation of China (Nos. 61761015 and 11664008) and the Natural Science Foundation of Guangxi (Nos. 2017GXNSFFA198011, 2018GXNSFFA050001, and 2017GXNSFDA198027) and High-Level Innovation Team and Outstanding Scholar Program of Guangxi Institutes.

References

[1] X. L. Chen, H. F. Zhou, L. A. Fang, X. B. LiuY. L. Wang Microwave dielectric properties and its compatibility with silver electrode of $Li_2MgTi_3O_8$ ceramics. J. Alloy. Compd. 2011, 509 (19): 5829-5832.

[2] K. G. Wang, H. F. Zhou, X. B. Liu, W. D. Sun, X. L. ChenH. Ruan A lithium aluminium borate composite microwave dielectric ceramic with low permittivity, near-zero shrinkage, and low sintering temperature. J. Eur. Ceram. Soc. 2019, 39 (4): 1122-1126.

[3] H. F. Zhou, X. H. Tan, J. Huang, N. Wang, G. C. FanX. L. Chen Phase structure, sintering behavior and adjustable microwave dielectric properties of $Mg_{1-x}Li_{2x}Ti_xO_{1+2x}$ solid solution ceramics. J. Alloy. Compd. 2017, 696: 1255-1259.

[4] H. B. Bafrooei, E. T. Nassaj, T. Ebadzadeh, C. F. Hu, A. Sayyadi-ShahrakiT. Kolodiazhnyi Sintering behavior and microwave dielectric characteristics of $ZnTiNb_2O_8$ ceramics achieved by reaction sintering of ZnO-TiO_2-Nb_2O_5 nanosized powders. Ceram. Int. 2016, 42 (2): 3296-3303.

[5] M. Bari, E. Taheri-NassajH. Taghipour-Armaki Phase Evolution, Microstructure, and Microwave Dielectric Properties of Reaction-Sintered $Li_2ZnTi_3O_8$ Ceramic Obtained Using Nanosized TiO_2 Reagent. J. Electron. Mater. 2015, 44 (10): 3670-3676.

[6] P. Gogoi, L. R. SinghD. Pamu Characterization of Zn doped $MgTiO_3$ ceramics: an approach for RF capacitor applications. J. Mater. Sci.-Mater. Electron. 2017, 28 (16): 11712-11721.

[7] W. T. Xie, Q. X. Jiang, Q. L. Cao, H. Q. Zhou, L. C. RenX. F. Luo Microwave dielectric properties of (1-*x*)$ZnNb_2O_6$-*x*$Ba(Zn_{1/3}Nb_{2/3})O_3$ compound ceramic with near zero temperature coefficient. J. Mater. Sci.-Mater. Electron. 2018, 29 (3): 2170-2174.

[8] E. A. Tugova, A. V. Travitskov, M. V. Tomkovich, V. V. SokolovE. A. Nenasheva Solid-Phase Synthesis and Dielectric Properties of Materials Based on $LaAlO_3$-$CaTiO_3$ System. Russ. J. Appl. Chem. 2017, 90 (11): 1738-1745.

[9] J. Jiang, D. H. Fang, C. Lu, Z. M. Dou, G. Wang, F. ZhangT. J. Zhang Solid-state reaction mechanism and microwave dielectric properties of $CaTiO_3$-$LaAlO_3$ ceramics. J. Alloy. Compd. 2015, 638: 443-447.

[10] G. Wang, J. Jiang, Z. M. Dou, F. ZhangT. J. Zhang Sintering behavior and microwave dielectric properties of $0.67CaTiO_{(3)}$-$0.33LaAlO_{(3)}$ ceramics modified by B_2O_3-Li_2O-Al_2O_3 and CeO_2. Ceram. Int. 2016, 42 (9): 11003-11009.

[11] D. Li, C. Y. Luo, Y. B. Xu, L. Wu, H. X. Wang, S. J. Shi, F. R. LingJ. Q. Yao The effect of optical pump on the absorption coefficient of $0.65CaTiO_{(3)}$-$0.35NdAlO_{(3)}$ ceramics in terahertz range. Opt. Mater. 2018, 75: 280-284.

[12] X. Y. Yang, X. H. Wang, M. Huang, S. P. ZhangL. T. Li Synthesis and characterization of $CaTiO_3$-$(Sm,Nd)AlO_3$ microwave ceramics via sol-gel method. J. Sol-Gel Sci. Technol. 2014, 69 (1): 61-66.

[13] M. H. Weng, C. T. Liauh, S. M. Lin, H. H. WangR. Y. Yang Sintering Behaviors, Microstructure, and Microwave Dielectric Properties of $CaTiO_3$-$LaAlO_3$ Ceramics Using CuO/B_2O_3 Additions. Materials 2019, 12 (24): 12.

[14] Z. M. Dou, G. Wang, J. Jiang, F. ZhangT. J. Zhang Understanding microwave dielectric properties of (*1*-x)$CaTiO_3$-x$LaAlO_{(3)}$ ceramics in terms of A/B-site ionic-parameters. J. Adv. Ceram. 2017, 6 (1): 20-26.

[15] Sintering Behavior and Microwave Dielectric Properties of (Ca, La)(Ti, Al)O_3 Ceramics.

[16] G. H. Hou, Z. H. WangF. Zhang Sintering behavior and microwave dielectric properties of (*1*-x)$CaTiO_3$-x$LaAlO_{(3)}$ ceramics. J. Rare Earths 2011, 29 (2): 160-163.

[17] P. Ruan, P. Liu, B. C. Guo, F. LiZ. F. Fu Microwave dielectric properties of ZnO-Nb_2O_5-*x*$TiO_{(2)}$ ceramics prepared by reaction-sintering process. J. Mater. Sci.-Mater. Electron. 2016, 27 (5): 4201-4205.

[18] G. Wang, D. N. Zhang, G. W. Gan, Y. Yang, Y. H. Rao, F. Xu, X. Huang, Y. L. Liao, J. Li, C. Liu, L. C. JinH. W. Zhang Synthesis, crystal structure and low loss of $Li_3Mg_2NbO_6$ ceramics by reaction sintering process. Ceram. Int. 2019, 45 (16): 19766-19770.

[19] G. G. Yao Synthesis and microwave dielectric properties of $Li_2ZnTi_3O_8$ ceramics by the reaction-sintering process. J. Ceram. Process. Res. 2015, 16 (1): 41-44.

[20] H. F. Zhou, H. Wang, Y. H. Chen, K. C. LiX. Yao Microwave Dielectric Properties of $BaTi_5O_{11}$ Ceramics Prepared by Reaction-Sintering Process with the Addition of CuO. J. Am. Ceram. Soc. 2008, 91 (10): 3444-3447.

[21] J. M. Li, P. Xu, T. QiuL. C. Yao Sintering characteristics and microwave dielectric properties of 0.5$Ca_{(0.6)}La_{(0.267)}TiO_{(3)}-0.5Ca(Mg_{1/3}Nb_{2/3})O_3$ ceramics prepared by

reaction-sintering process. J. Rare Earths 2018, 36 (4): 404-408.

[22] J. D. Guo, W. B. Ma, M. J. Ma, H. D. Zhao, Y. X. YangJ. F. Gao Sintering characteristic and microwave dielectric properties of ultra-low loss $Li_2Mg_3TiO_6$ ceramic prepared by reaction-sintering process. J. Mater. Sci.-Mater. Electron. 2018, 29 (5): 3640-3647.

[23] B. C. Guo, P. Liu, Z. F. Fu, P. RuanX. J. Bai Effect of Preparation Methods on Microstructures and Microwave Dielectric Properties of $CdWO_4$ Ceramics. Integr. Ferroelectr. 2015, 167 (1): 107-114.

[24] L. He, H. T. Yu, M. S. Zeng, E. Z. Li, J. S. LiuS. R. Zhang Phase compositions and microwave dielectric properties of $MgTiO_3$-based ceramics obtained by reaction-sintering method. J. Electroceram. 2018, 40 (4): 360-364.

[25] P. Riazikhoei, F. AzoughR. Freer The influence of $ZnNb_2O_6$ on the microwave dielectric properties of $ZM_{(2)}O_{(6)}$ ceramics. J. Am. Ceram. Soc. 2006, 89 (1): 216-223.

[26] M. J. Wu, Y. C. Zhang, J. D. ChenM. Q. Xiang Microwave dielectric properties of sol-gel derived $NiZrNb_2O_8$ ceramics. J. Alloy. Compd. 2018, 747: 394-400.

[27] C. F. Xing, Y. H. Zhang, B. J. Tao, H. T. WuY. Y. Zhou Crystal structure, infrared spectra and microwave dielectric properties of low-firing $La_2Zr_3(MoO_4)_{(9)}$ ceramics prepared by reaction-sintering process. Ceram. Int. 2019, 45 (17): 22376-22382.

[28] H. T. Yu, T. Luo, L. HeJ. S. Liu Effect of ZnO on Mg_2TiO_4-$MgTiO_3$-$CaTiO_3$ microwave dielectric ceramics prepared by reaction sintering route. Adv. Appl. Ceram. 2019, 118 (3): 98-105.

[29] L. M. Zhang, Y. Chang, M. Xin, X. F. Luo, H. J. Tao, Y. Fu, P. Z. LiH. Q. Zhou Synthesis of $0.65CaTiO_{(3)}$-$0.35SmAlO_{(3)}$ ceramics and effects of La_2O_3/SrO doping on their microwave dielectric properties. J. Mater. Sci.-Mater. Electron. 2018, 29 (24): 21205-21212.

[30] H. F. Zhou, W. D. Sun, X. B. Liu, K. G. Wang, H. RuanX. L. Chen Microwave dielectric properties of $LiCa_3ZnV_3O_{12}$ and $NaCa_2Mg_2V_3O_{12}$ ceramics prepared by reaction-sintering. Ceram. Int. 2019, 45 (2): 2629-2634.

Figure Captions

Figure 1. XRD patterns of CTLA and CTNA ceramics sintered at 1100 to 1575°C for 6h.

Figure 2. Rietveld refinement of the room temperature XRD patterns of $CaTiO_3$-$LnAlO_3$(Ln=La, Nd) ceramic (CTLA: *Rp* = 4.09%, *Rwp* = 7.43%, χ^2 =15.55; CTNA: R_{wp}= 7.57%, R_p = 4.17%, χ^2 = 11.08).

Figure 3. SEM micrographs of $CaTiO_3$-$LnAlO_3$(Ln=La, Nd) ceramics sintered at 1475 to 1550°C for 6h.

Figure 4. The curves of ρ, ε_r, $Q\times f$ and τ_f of $CaTiO_3$-$LnAlO_3$(Ln=La, Nd) ceramics as a function of the sintering temperature.

Table. 1 Atomic percentage of $CaTiO_3$-$LnAlO_3$(Ln=La, Nd) quantified from EDS spectra

Element Atomic (%)	***Ca***	***Ti***	***La/Nd***	***Al***	***O***
CTLA	18.76	20.09	10.19	10.09	40.87
CTNA	19.85	20.77	9.94	7.76	41.68

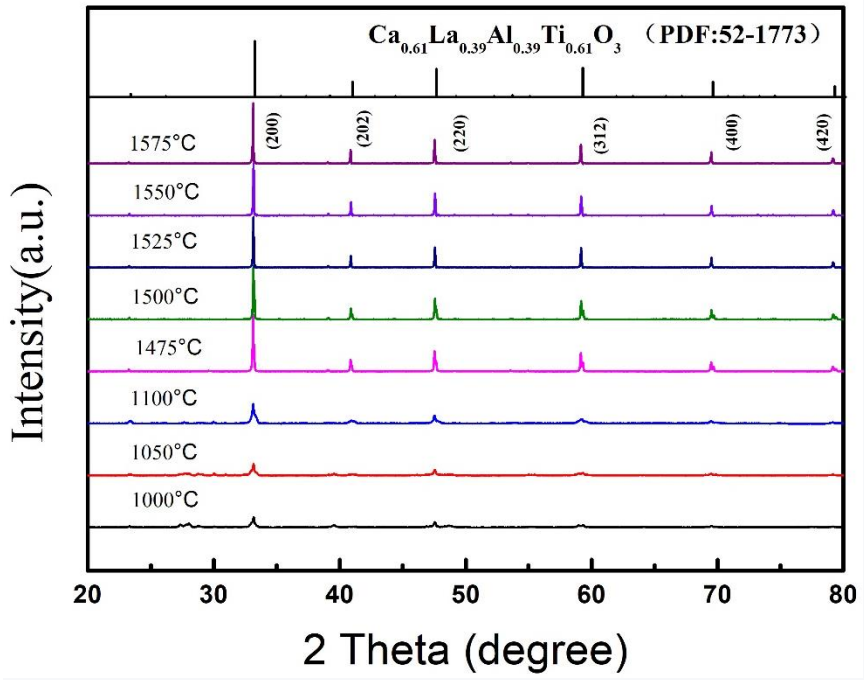
Ca0.61La0.39Al0.39Ti0.61O3 （PDF:52-1773）
(200)
(202)
(220)
(312)
(400)
(420)
1575°C
1550°C
1525°C
1500°C
1475°C
1100°C
1050°C
1000°C
Intensity(a.u.)
20
30
40
50
60
70
80
2 Theta (degree)

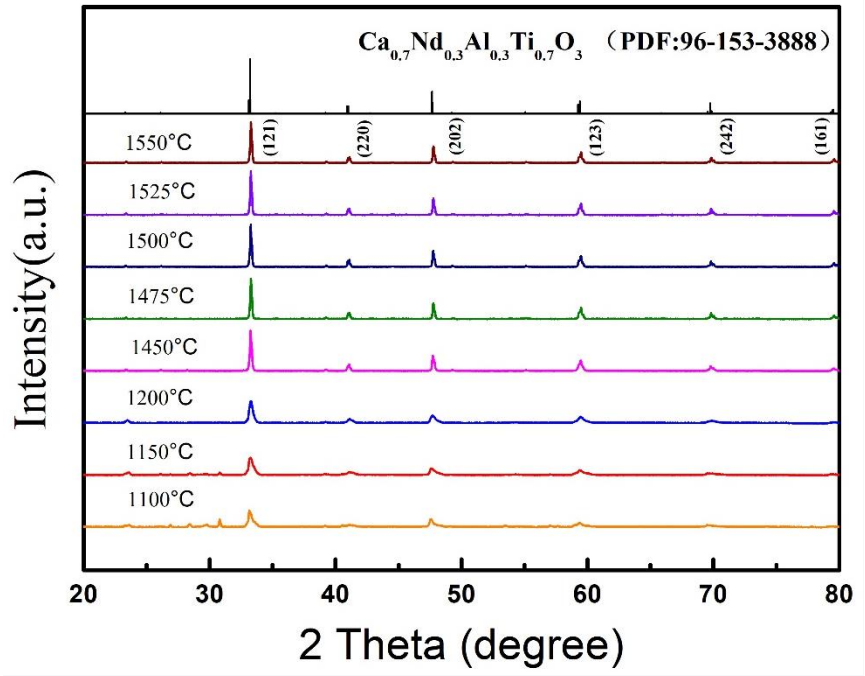
Ca0.7Nd0.3Al0.3Ti0.7O3 （PDF:96-153-3888）
(121)
(220)
(202)
(123)
(242)
(161)
1550°C
1525°C
1500°C
1475°C
1450°C
1200°C
1150°C
1100°C
Intensity(a.u.)
20
30
40
50
60
70
80
2 Theta (degree)

Figure 1

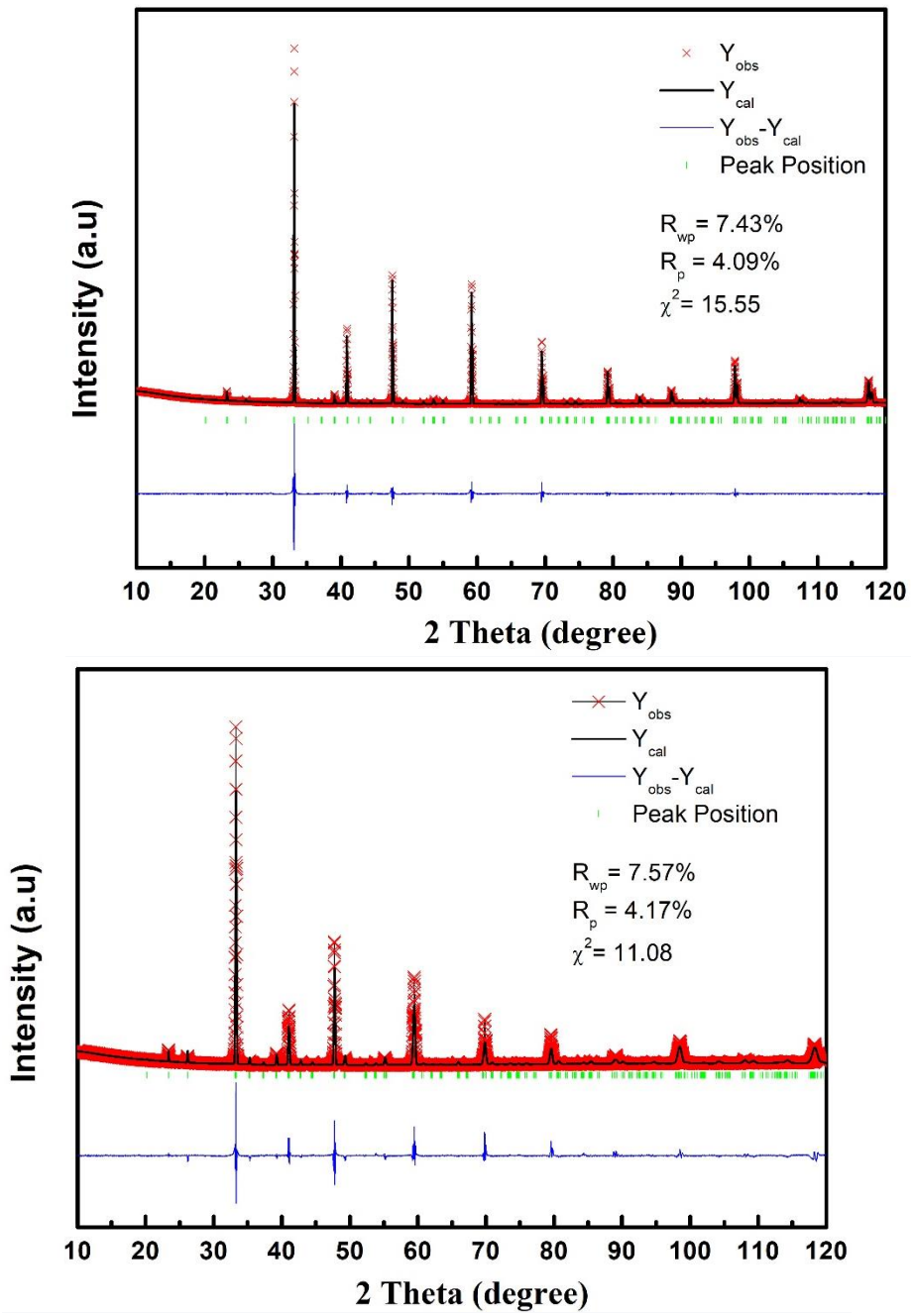
Y obs
Y cal
Y obs-Y cal
Peak Position
R wp = 7.43%
R p = 4.09%
χ2 = 15.55
Intensity (a.u)
10 20 30 40 50 60 70 80 90 100 110 120
2 Theta (degree)
Y obs
Y cal
Y obs-Y cal
Peak Position
R wp = 7.57%
R p = 4.17%
χ2 = 11.08
Intensity (a.u)
10 20 30 40 50 60 70 80 90 100 110 120
2 Theta (degree)

Figure 2

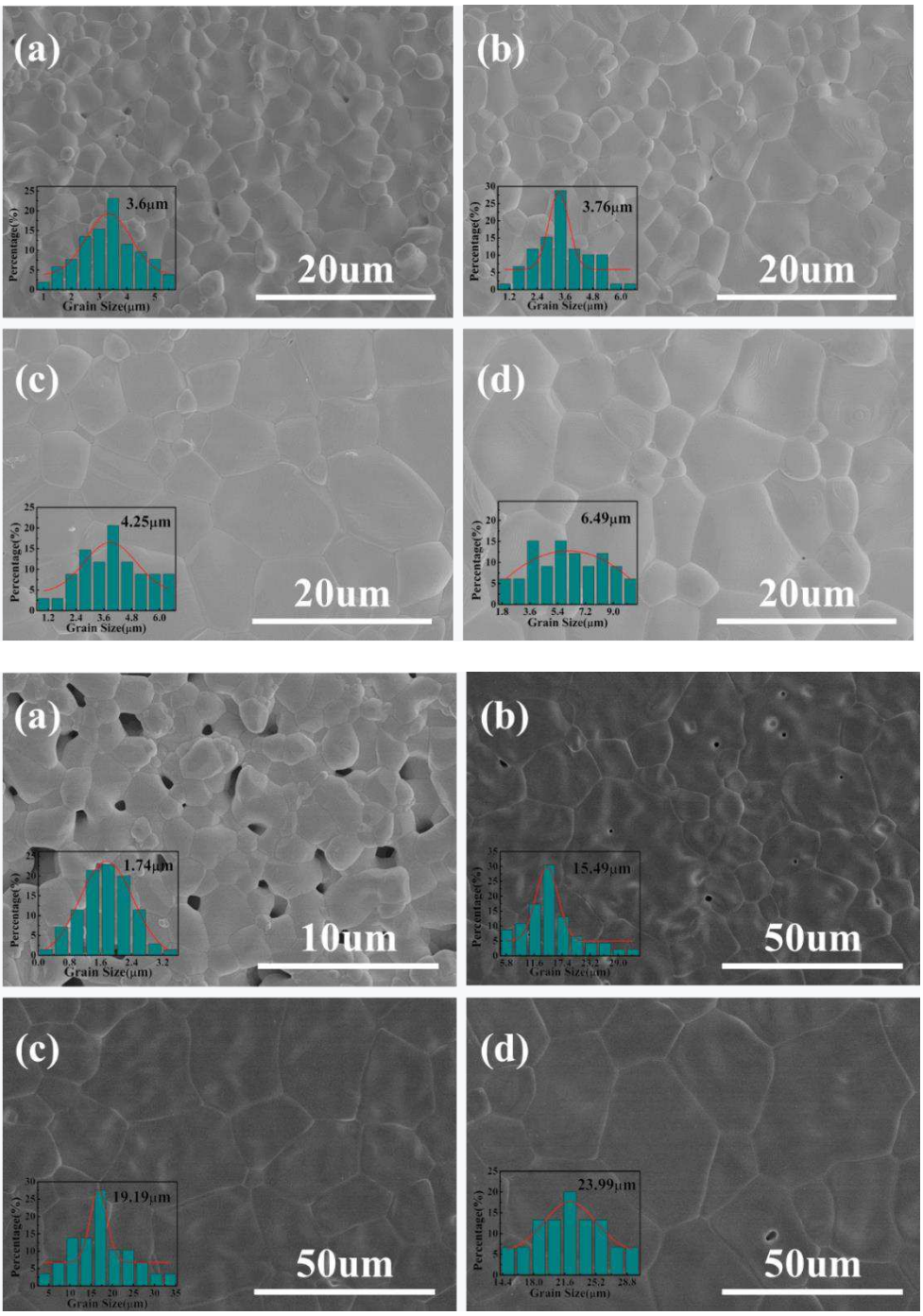
(a)
3.6μm
Percentage(%)
Grain Size(μm)
20um
(b)
3.76μm
Percentage(%)
Grain Size(μm)
20um
(c)
4.25μm
Percentage(%)
Grain Size(μm)
20um
(d)
6.49μm
Percentage(%)
Grain Size(μm)
20um
(a)
1.74μm
Percentage(%)
Grain Size(μm)
10um
(b)
15.49μm
Percentage(%)
Grain Size(μm)
50um
(c)
19.19μm
Percentage(%)
Grain Size(μm)
50um
(d)
23.99μm
Percentage(%)
Grain Size(μm)
50um

Figure 3

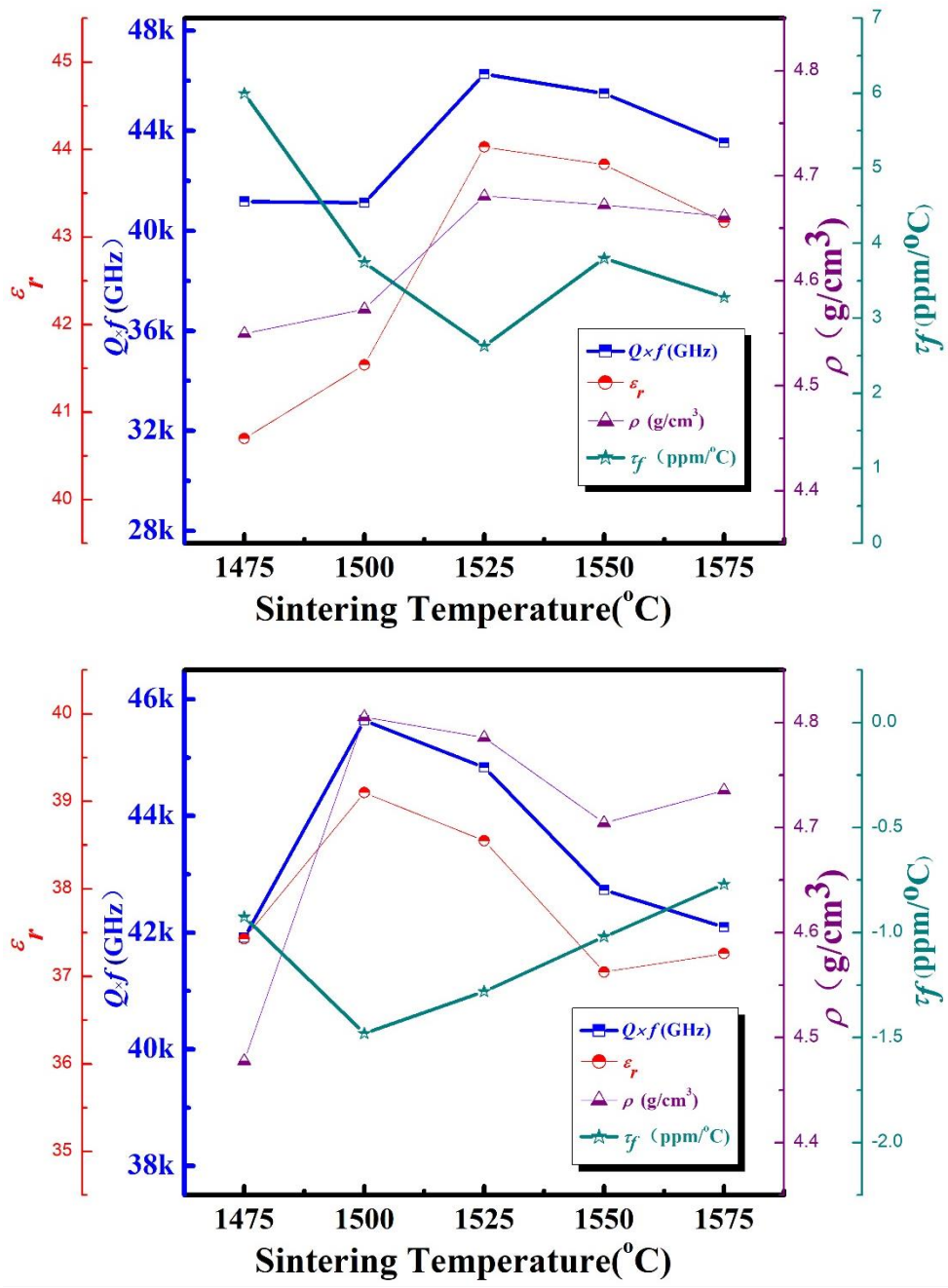
48k
44k
40k
36k
32k
28k
45
44
43
42
41
40
ε_r
$Q\times f$(GHz)
4.8
4.7
4.6
4.5
4.4
ρ (g/cm^3)
7
6
5
4
3
2
1
0
τ_f(ppm/^{o}C)
$Q\times f$(GHz)
ε_r
ρ (g/cm^3)
τ_f (ppm/^{o}C)
1475
1500
1525
1550
1575
Sintering Temperature(^{o}C)
46k
44k
42k
40k
38k
40
39
38
37
36
35
ε_r
$Q\times f$(GHz)
4.8
4.7
4.6
4.5
4.4
ρ (g/cm^3)
0.0
-0.5
-1.0
-1.5
-2.0
τ_f(ppm/^{o}C)
$Q\times f$(GHz)
ε_r
ρ (g/cm^3)
τ_f (ppm/^{o}C)
1475
1500
1525
1550
1575
Sintering Temperature(^{o}C)

Figure 4

Figures

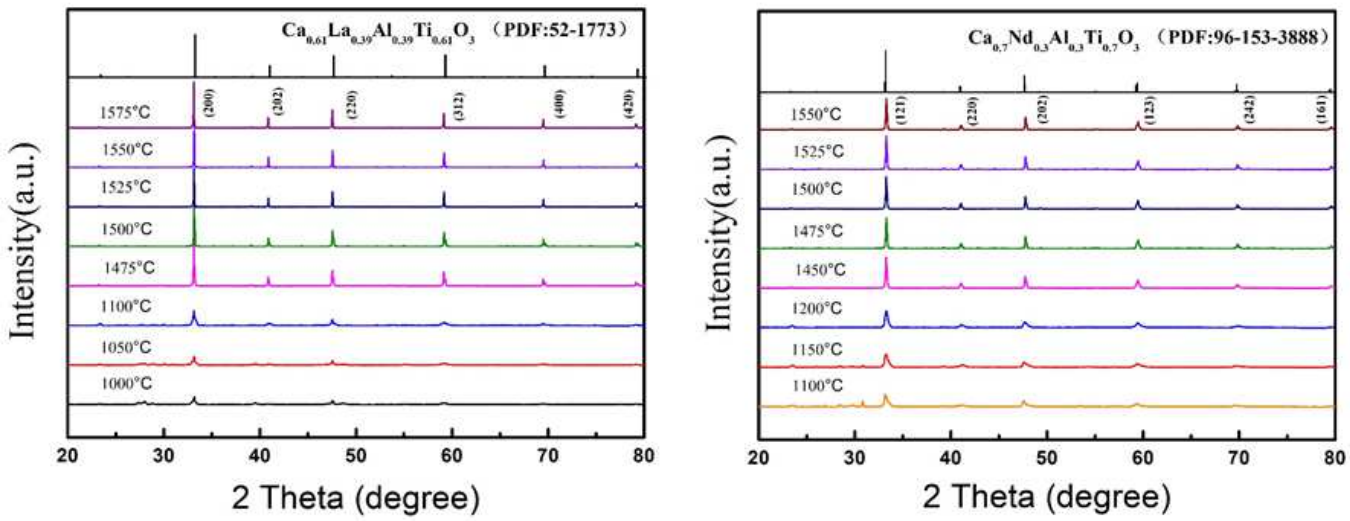

Figure 1

XRD patterns of CTLA and CTNA ceramics sintered at 1100 to 1575°C for 6h.

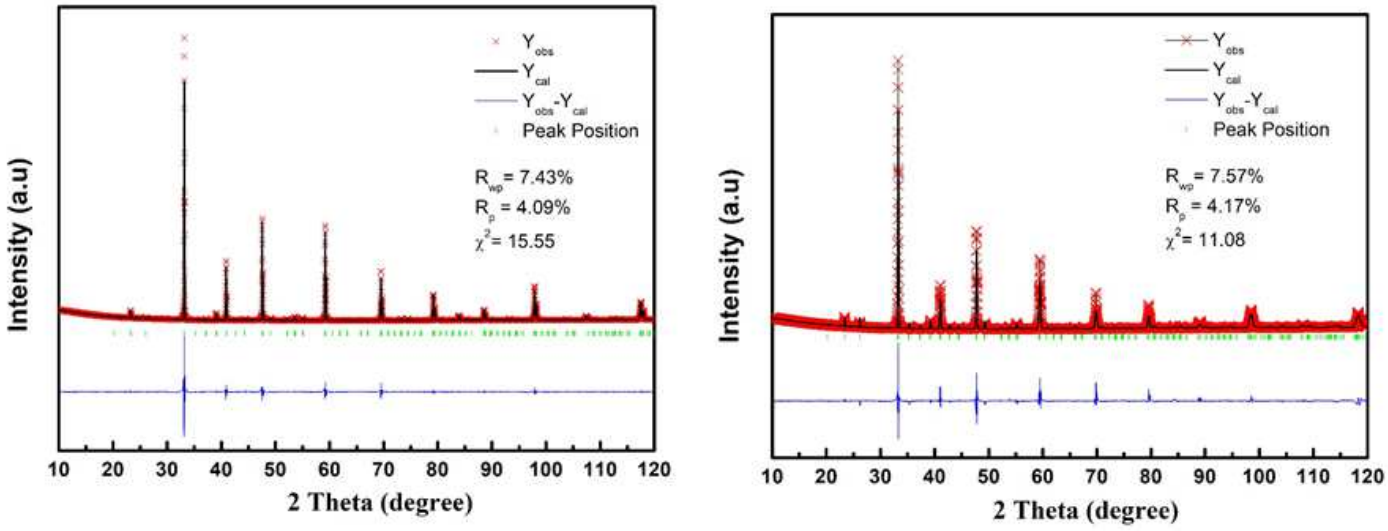

Figure 2

Rietveld refinement of the room temperature XRD patterns of CaTiO3-LnAlO3(Ln=La, Nd) ceramic (CTLA: Rp = 4.09%, Rwp = 7.43%, 2 =15.55; CTNA: Rwp= 7.57%, Rp = 4.17%, 2 = 11.08).

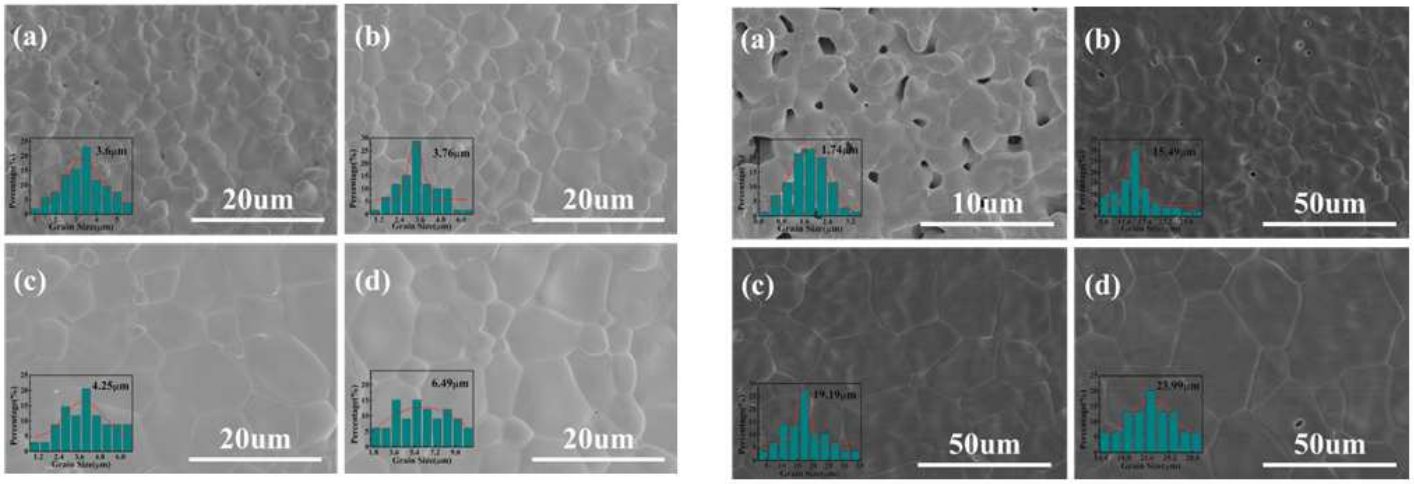

Figure 3

SEM micrographs of CaTiO3-LnAlO3(Ln=La, Nd) ceramics sintered at 1475 to 1550°C for 6h.

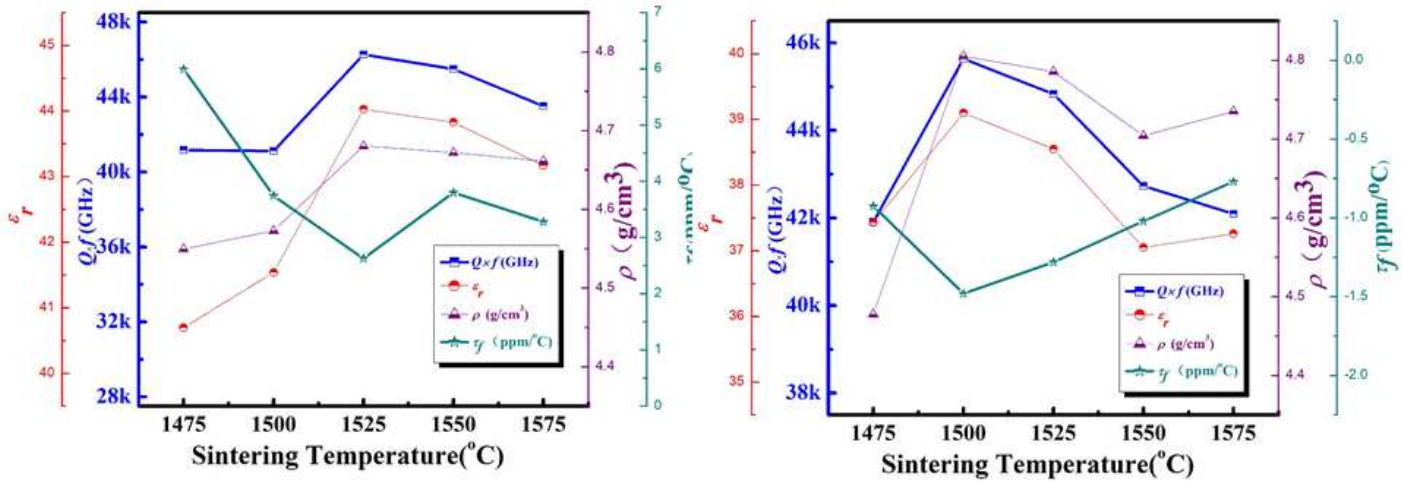

Figure 4

The curves of ρ, εr, Q×f and τf of CaTiO3-LnAlO3(Ln=La, Nd) ceramics as a function of the sintering temperature.